6 October 2000

Chemical Physics Letters 328 (2000) 431–436

CHEMICAL PHYSICS LETTERS

www.elsevier.nl/locate/cplett

A new diagnostic for open-shell coupled-cluster theory

Matthew L. Leininger [a,*], Ida M.B. Nielsen [a], T. Daniel Crawford [b], Curtis L. Janssen [a,1]

[a] *Sandia National Laboratories, Livermore, CA 94551-0969, USA*

[b] *Department of Chemistry, Virginia Polytechnic Institute and State University, Blacksburg, VA 24061-0212, USA*

Received 3 April 2000; received in final form 8 August 2000

Abstract

We present a new diagnostic for open-shell coupled-cluster theory, readily computed from the single substitution amplitudes in the CCSD wavefunction. The new diagnostic, D_1(ROCCSD), is designed to be comparable to the previously proposed D_1(CCSD) diagnostic. Unlike other approaches, the D_1 diagnostics are independent of system size and have the same invariance properties as the energy with respect to orbital rotations. Calibration of the D_1(ROCCSD) diagnostic on 34 molecular systems indicates that for values of D_1(ROCCSD) of 0.025 or below the quality of the CCSD results are, in general, excellent, whereas values larger than 0.025 signal inadequacies in the CCSD approach.

1. Introduction

Coupled-cluster theory [1–3] is among the most reliable methods for including the electron correlation effects in molecular systems. The most efficient coupled-cluster approaches are based on a single-reference Hartree–Fock wavefunction, and generally perform better for systems well described by a single electronic configuration. When used in conjuction with basis set extrapolation techniques, the coupled-cluster methods can provide molecular properties for small-to-medium sized molecules to near chemical accuracy (~1 kcal/mol) [4–10]. For determining the quality of single-reference coupled-cluster results, diagnostics that assess the quality of the reference wavefunction are extremely valuable. Such diagnostics are particularly important for studying large systems where improving the level of theory, by complete basis set extrapolation or higher levels of correlation, is too computationally expensive, and the results from a single computation have to be trusted. We have previously proposed diagnostics for coupled-cluster and second-order many-body perturbation theory based on closed-shell reference wavefunctions [11,12]. We herein propose a comparable diagnostic for coupled-cluster methods based on spin-restricted open-shell reference wavefunctions.

2. Theory

A diagnostic for open-shell coupled-cluster theory should have several properties: the diagnostic must be easily computed so that its computational cost is essentially insignificant

* Corresponding author. Fax: +1-925-294-2234.

E-mail addresses: mlleini@ca.sandia.gov (M.L. Leininger), ibniels@ca.sandia.gov (I.M.B. Nielsen), crawdad@ut.edu (T.D. Crawford), cljanss@ca.sandia.gov (C.L. Janssen).

[1] Fax: +1-925-294-2234.

0009-2614/00/$ - see front matter
PII: S0009-2614(00)00966-0

compared to the cost of an energy calculation; it should reflect the quality of the wavefunction [2]; it should be independent of the size of the system (size-intensive) so that diagnostics for various systems can be meaningfully compared; and it should have the same invariance properties as the energy with respect to orbital rotations. We have previously pointed out the problems with using diagnostics based on the Frobenius matrix norm, like the popular $\mathscr{T}_1$ diagnostic [11,12]. Here we focus on developing a singles diagnostic which has the above mentioned properties, which represents the spatial orbital relaxation due to the coupled-cluster wavefunction, and which is based on the singles amplitude matrix 2-norm [13].

In the spatial orbital basis the single substitution part of the open-shell cluster operator can be written

$$T_1 = t_{i\alpha}^{a\alpha} a_{a\alpha}^{\dagger} a_{i\alpha} + t_{i\beta}^{a\beta} a_{a\beta}^{\dagger} a_{i\beta} + t_{x\alpha}^{a\alpha} a_{a\alpha}^{\dagger} a_{x\alpha} + t_{i\beta}^{x\beta} a_{x\beta}^{\dagger} a_{i\beta}, \tag{1}$$

where a, i, and x designate unoccupied, doubly occupied, and singly occupied orbitals, respectively. To make it clear which parts of this operator preserve spin symmetry and which parts break it, we will rewrite T_1 in terms of spin-symmetry preserving unitary group generators, $E_{pq} = a_{p\alpha}^{\dagger} a_{q\alpha} + a_{p\beta}^{\dagger} a_{q\beta}$, and the spin-symmetry breaking operators, $A_{pq} = a_{p\alpha}^{\dagger} a_{q\alpha} - a_{p\beta}^{\dagger} a_{q\beta}$

$$T_1 = r_i^a E_{ai} + u_i^a A_{ai} + r_x^a E_{ax} + u_x^a A_{ax} + r_i^x E_{xi} + u_i^x A_{xi}, \tag{2}$$

where

$$\begin{aligned} r_i^a &= \left(t_{i\alpha}^{a\alpha} + t_{i\beta}^{a\beta}\right)/2, \\ u_i^a &= \left(t_{i\alpha}^{a\alpha} - t_{i\beta}^{a\beta}\right)/2, \\ r_i^x &= t_{i\beta}^{x\beta}/2, \\ u_i^x &= -t_{i\beta}^{x\beta}/2, \\ r_x^a &= t_{x\alpha}^{a\alpha}/2, \\ u_x^a &= t_{x\alpha}^{a\alpha}/2. \end{aligned} \tag{3}$$

[2] It should be noted that the quality of the single-determinant reference wavefunction is dependent upon both orbital relaxation and multireference effects, which themselves are inherently coupled. The D_1 diagnostic developed here is intended to serve as a measure primarily of the former, though some estimate of the latter is naturally expected as well.

We then define the new diagnostic in terms of the matrix 2-norms [13] of the unitary group generator coefficients

$$D_1(\mathrm{ROCCSD}) = \max\left(\|r_i^a\|_2, \|r_x^a\|_2, \|r_i^x\|_2\right), \tag{4}$$

thus including only orbital rotations that preserve spin symmetry. The 2-norm of a matrix R is defined as the maximum Euclidean norm of the vectors formed by multiplication of R with a unit vector $\boldsymbol{x}$. The matrix 2-norm is easily computed from

$$\|\mathbf{R}\|_2 = \sqrt{\lambda_{\max}} = \sigma_{\max}, \tag{5}$$

where $\lambda_{\max}$ is the largest eigenvalue of the matrix $\mathbf{R}\mathbf{R}^{\mathrm{T}}$ and $\sigma_{\max}$ is the largest singular value of $\mathbf{R}$. For the special case with no open-shell orbitals, $D_1(\mathrm{ROCCSD})$ is equivalent to the previously proposed diagnostic, $D_1(\mathrm{CCSD})$ [11].

A restricted open-shell diagnostic could also be defined to be the 2-norm of the matrix corresponding to the spin-restricted single substitution amplitudes

$$t_r = \begin{bmatrix} r_i^a & r_x^a \\ r_i^x & 0 \end{bmatrix}, \tag{6}$$

where the columns correspond to orbitals with nonzero occupancy and the rows to orbitals with less than double occupancy in the reference. A diagnostic computed in this way is always larger than or equal to $D_1(\mathrm{ROCCSD})$. This can be proven Ref. [13], using Corollary 8.6.3. Computing the 2-norm of this matrix is equivalent to finding the largest individual element obtainable by distinct unitary transforms of the row and column bases. However, that allows too much flexibility, since the open-shell, doubly occupied, and virtual orbital blocks would have complete freedom to mix. Thus, the diagnostic would not correspond to the maximum single substitution amplitude of any possible rotated set of orbitals that preserve the energy.

In previous work, we were able to relate the closed-shell diagnostic, $D_1(\mathrm{CCSD})$, to the $\mathscr{T}_1$ diagnostic with the relation $\sqrt{2}\mathscr{T}_1 \leqslant D_1(\mathrm{CCSD})$, but no similar relationship holds for $D_1(\mathrm{ROCCSD})$ and the open-shell $\mathscr{T}_1$. The open-shell $\mathscr{T}_1$ is most commonly defined to be $\mathscr{T}_1 = \|t_{\mathscr{T}_1}\|_{\mathrm{F}}/\sqrt{n_{\mathrm{corr}}}$ [14], where

$$t_{\mathscr{T}_1} = \begin{bmatrix} r_i^a & \sqrt{2}\, r_x^a \\ \sqrt{2}\, r_i^x & 0 \end{bmatrix}. \quad (7)$$

We note that the blocks containing open-shell orbitals in t_r and $t_{\mathscr{T}_1}$ differ by a factor of $\sqrt{2}$. This factor originates from the fact that $\mathscr{T}_1$ was formulated from a coupled-cluster approach using a symmetric spin-orbital basis [14]. Coupled-cluster theory does not specify any particular scaling factors for the three blocks of $t_{\mathscr{T}_1}$; however, we view our diagnostic as a measure of spatial orbital relaxation, and it is therefore natural to use the coefficients of the unitary group generators to develop the diagnostic. In both standard spin-orbital and symmetrized open-shell formulations of CCSD, the coefficients of the unitary group generators are given by t_r. This choice seems reasonable when comparing the diagnostics for the $^3B_1$ and $^1A_1$ states of CH_2. Intuitively, orbital relaxation in the $^1A_1$ state should be more significant because of its inherent coupling to the important pair excitation from the high-lying doubly occupied a_1 to the low-lying unoccupied b_1 orbital. We computed the diagnostics for these states of CH_2 using the frozen core approximation, the cc-pVTZ basis set, and the experimental geometries. We found that $\mathscr{T}_1 =$ 0.0107 and 0.0091 for the triplet and singlet, respectively, whereas the D_1(ROCCSD) diagnostic takes on the values 0.0127 and 0.0194. If the factors of $\sqrt{2}$ had been included in our definition of D_1(ROCCSD), then our value for the $^3B_1$ state would have been 0.0179, which is rather close to the value of 0.0194 for the $^1A_1$ state.

3. Applications

The standard cc-pVTZ correlation consistent basis sets of Dunning et al. [15,16] containing pure spherical harmonic manifolds were employed throughout the present study. In order to gauge the reliability of the new diagnostic, ROHF-CCSD and ROHF-CCSD(T) optimum geometries and harmonic vibrational frequencies were computed using the ACESII [17] package with all electrons correlated. The geometries were considered to have converged when the residual internal coordinate gradients were less than 10^{-6} a.u. All harmonic vibrational frequencies were calculated via finite differences of analytic gradients. The reported D_1(ROCCSD) and $\mathscr{T}_1$ [18,19] diagnostics were computed from the ROHF-CCSD singles amplitudes obtained from the PSI3 program package [20] at the corresponding optimized geometry. All electrons were included in the computations of D_1(ROCCSD), whereas the $\mathscr{T}_1$ diagnostics were computed using only the number of valence electrons as previously recommended [18,19]. As found in our earlier closed-shell studies [11,12], the D_1 diagnostics are only negligibly affected by whether the core electrons are frozen or explicitly correlated.

A 34 molecule test set was employed to calibrate the proposed diagnostic against the errors in the CCSD optimized geometries and harmonic vibrational frequencies. The molecular test set and diagnostics are shown in Table 1 along with the ROHF-CCSD, ROHF-CCSD(T), and experimental geometries and frequencies. For our test set, the ROHF-CCSD(T) method, in general, accurately reproduces the available experimental data, and therefore its results are taken as the standard to which the ROHF-CCSD method is calibrated. This also allows a better assessment of the correlation procedure since the errors due to basis set deficiency and neglect of core correlation are expected to be similar for the two methods.

The percent relative error of the ROHF-CCSD bond lengths is plotted in Fig. 1 as a function of the D_1(ROCCSD) diagnostic values. A similar plot for harmonic vibrational frequencies is shown in Fig. 2. The magnitude of the errors is clearly correlated with the size of the diagnostic. For molecules with small diagnostics, D_1(ROCCSD) $\leqslant 0.025$, the errors in predicted bond lengths and frequencies are all less than 0.5% and 2.0%, respectively. Values of D_1(ROCCSD) > 0.025 signal the inadequacy of CCSD theory. The only exception to this bound is X $^3\Sigma_g^+$ O_2 (labeled A in Figs. 1 and 2) which has a diagnostic value of 0.0125 but bond length and frequency errors of 1.2% and 5.6%, respectively. This can be attributed to several large doubles amplitudes in the CCSD wavefunction that are not accounted for in the present diagnostic. The substantial errors for X $^2\Pi_g$ O_2^+ (labeled B in Figs. 1 and 2) are also due in part to

Table 1
Coupled-cluster diagnostics, bond distances (Å) and harmonic vibrational frequencies (cm^{-1}) in the cc-pVTZ basis

Molecule	D_1	$\mathscr{T}_1$	r_e			ω_e		
	CCSD	CCSD	CCSD	CCSD(T)	Expt.	CCSD	CCSD(T)	Expt.[a]
X $^2A'$ CCF	0.2782	0.1032	1.261,1.266	1.262,1.274		1686,1002,420	1554,966,444	
a $^1\Sigma^+$ BN	0.2097	0.0764	1.273	1.268	1.275[d]	1714	1746	1705[b]
X $^1\Sigma^+$ CN^+	0.1892	0.0698	1.175	1.163	1.1729	2074	1991	2033
X $^2\Sigma^+$ CN	0.1070	0.0530	1.165	1.175	1.1718	2158	2074	2068
X $^2\Sigma^+$ NSi	0.1037	0.0600	1.573	1.587	1.571	1189	1134	1151
a $^3\Pi$ CN^+	0.1002	0.0533	1.231	1.245	1.241[b]	1818	1718	1711[b]
X $^2A''$ HOO	0.0869	0.0354	0.967,1.323	0.970,1.332	0.9708,1.33051	3739,1472,1177	3690,1442,1139	
X $^1\Sigma_g^+$ C_2	0.0861	0.0387	1.242	1.245	1.2425	1906	1871	1855
X $^3\Pi$ BN	0.0597	0.0353	1.318	1.329	1.281	1592	1521	1515
X $^2\Pi_{1/2}$ CCl	0.0564	0.0239	1.655	1.659	1.645	887	876	867
X $^2\Pi$ CCO^-	0.0535	0.0247	1.295,1.215	1.303,1.222	1.308,1.221	1998,1209,500(2)	1951,1172,468(2)	
X $^2\Sigma^+$CP	0.0511	0.0310	1.559	1.573	1.562	1292	1236	1240
X $^2\Pi$ ClS	0.0477	0.0211	1.996	2.001		581	572	
X $^2\Pi_r$ CF	0.0470	0.0189	1.268	1.273	1.2718	1359	1332	1308
X $^2\Pi$ PS	0.0455	0.0257	1.905	1.919	1.900	766	733	739
X $^2\Sigma^+$ BS	0.0454	0.0263	1.609	1.618	1.6092	1215	1181	1180
X $^2\Sigma^+$ BO	0.0451	0.0255	1.201	1.209	1.205	1949	1886	1886
X $^2\Sigma^+$ CO^+	0.0429	0.0280	1.110	1.120	1.1151	2319	2210	2214
X $^2\Pi_r$ NO	0.0417	0.0203	1.144	1.153	1.15077	2003	1919	1904
a $^1\Delta_g$ O_2	0.0401	0.0139	1.205	1.222	1.2156	1609	1492	1484
X $^3\Sigma^-$ NF	0.0388	0.0236	1.309	1.316	1.3169	1196	1163	1141
D $^3\Pi_u$ Si_2	0.0370	0.0221	2.158	2.170	2.155	568	551	511
X $^2\Pi_r$ CH	0.0342	0.0162	1.112	1.114	1.1199	2889	2871	2859
X $^2\Pi$ HCP^+	0.0342	0.0153	1.075,1.596	1.077,1.607	0.996,1.559[d]	3310,1207,684(2)	3285,1165,664(2)	
a $^3\Pi_u$ C_2	0.0319	0.0198	1.305	1.314	1.3119	1701	1655	1641
X $^2\Pi_g$ O_2^+	0.0317	0.0113	1.105	1.117	1.1164	2054	1932	1905
X $^2\Sigma_g^+$ N_2^+	0.0283	0.0192	1.110	1.119	1.11642	2300	2214	2207
X $^2\Sigma^-$ PCl	0.0259	0.0171	2.033	2.036		556	550	557
X $^3\Sigma^-$ FP	0.0225	0.0161	1.597	1.602	1.589	867	852	847
a $^1A_1$ CH_2	0.0188	0.0090	1.103	1.104	1.1112[c]	3007,2963,1433	2991,2945,1417	2839,2787,1351[c]
X $^2B_1$ PH_2	0.0184	0.0109	1.417	1.419	1.418[d]	2420,2411,1144	2402,2392,1131	
X $^2B_1$ H_2S^+	0.0143	0.0087	1.355	1.358	1.358[d]	2624,2620,1203	2603,2598,1190	
X $^3B_1$ CH_2	0.0130	0.0109	1.072	1.073	1.0794[c]	3391,3190,1112	3389,3186,1100	3236,3015,972[c]
X $^3\Sigma_g^+$ O_2	0.0125	0.0064	1.196	1.209	1.20752	1687	1597	1580
X $^2\Pi_i$ OH	0.0097	0.0057	0.967	0.969	0.96966	3797	3763	3738
X $^2A_2''$ CH_3	0.0092	0.0054	1.074	1.075	1.0767	3319(2),3161 1441(2),507	3304(2),3146 1432(2),510	
X $^2B_1$ NH_2	0.0092	0.0058	1.022	1.024	1.024[d]	3508,3420,1565	3478,3389,1555	
X $^3\Sigma^-$ OH^+	0.0064	0.0054	1.026	1.028	1.0289	3174	3148	3113

[a] Experimental values obtained from Refs. [21,22].
[b] Complete basis set limit CMRCI results from Ref. [23].
[c] MORBID fit to experimental data from Ref. [24].
[d] r_0 Structure.

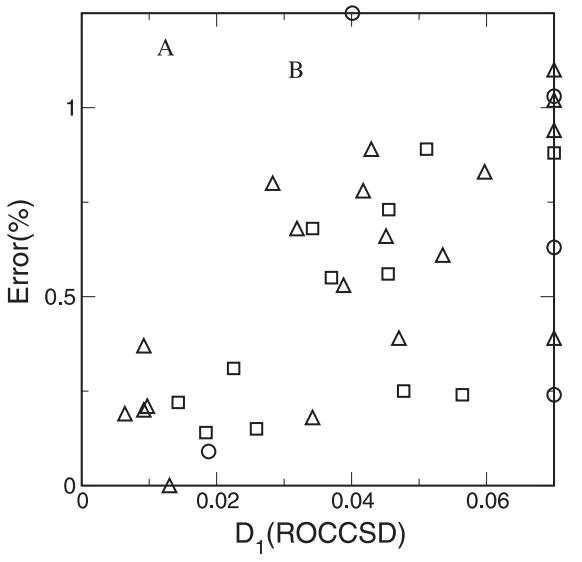

Fig. 1. cc-pVTZ CCSD bond errors relative to cc-pVTZ CCSD(T) values plotted against the D_1 diagnostics; errors are expressed as percentages of the CCSD(T) values, and only the largest error is shown for each molecule. Molecules containing second-row atoms are plotted with squares, other molecules with triangles; all singlet states are plotted with circles.

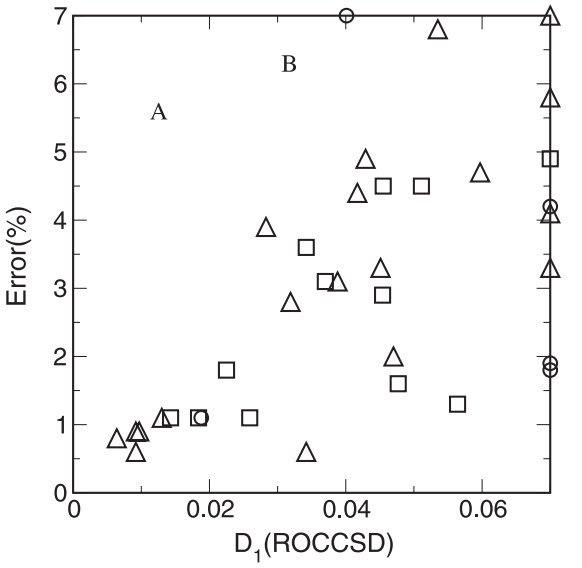

Fig. 2. cc-pVTZ CCSD errors in harmonic vibrational frequencies relative to cc-pVTZ CCSD(T) values plotted against the D_1 diagnostics; errors are expressed as percentages of the CCSD(T) values, and only the largest error is shown for each molecule. Molecules containing second-row atoms are plotted with squares, other molecules with triangles; all singlet states are plotted with circles.

large doubles amplitudes, although for this case the D_1(ROCCSD) diagnostic is above the recommended 0.025 cut-off. A doubles diagnostic [12] complementary to D_1(ROCCSD) is clearly necessary for these cases and will be considered in future work.

Table 2 displays the experimental, CCSD, and CCSD(T) singlet–triplet (ST) splittings for BN, CN^+, C_2, O_2, and CH_2, as well as the CCSD errors relative to experiment. For the ST splittings we do not consider the CCSD errors relative to the CCSD(T) values because the CCSD(T) values in some cases differ significantly from the experimental values. Overall, the D_1 diagnostics correlate well with the CCSD error in ST splittings. For O_2, both the CCSD and CCSD(T) ST splittings differ from the experimental value by more than 2500 cm^{-1}, indicating that the coupled-cluster methods are having difficulties describing this molecular system. These difficulties are mainly due to the inherent two-reference character of $^1\Delta_g$ O_2. Even

Table 2
Coupled-cluster diagnostics and CCSD, CCSD(T), and experimental singlet–triplet splittings (cm^{-1})

Molecule	D_1(ROCCSD)[a]	D_1(CCSD)[b]	$\mathscr{T}_1$[a]	$\mathscr{T}_1$[b]	CCSD[c]	CCSD(T)[c]	Expt.[c]	CCSD error(%)[d]
BN	0.0597	0.2097	0.0353	0.0764	−4338	328	190[e]	2383
CN^+	0.1002	0.1892	0.0533	0.0698	−3626	1814	880[e]	512
C_2	0.0319	0.0861	0.0198	0.0387	−2652	839	716	470
O_2	0.0125	0.0401	0.0064	0.0139	11270	10499	7918	42
CH_2	0.0130	0.0188	0.0109	0.0090	4133	3816	3278	26

[a] High-spin open-shell triplet diagnostics.
[b] Closed-shell singlet diagnostics.
[c] Computed relative to experimental ground states.
[d] Error relative to experiment.
[e] Complete basis set limit CMRCI results from Ref. [23].

the highly correlated single-reference CCSDT method yields a ST splitting of 9524 cm^{-1}, some 1606 cm^{-1} above the experimental value. It is worth noting that the D_1(CCSD) diagnostic reveals that the CCSD results for O_2 are suspect, while the $\mathscr{T}_1$ diagnostic is below the recommended cut-off of 0.020 [18,19].

4. Concluding remarks

An improved diagnostic for open-shell coupled-cluster theory has been proposed which is computed from the singles substitution amplitudes obtained from a CCSD procedure. The new diagnostic, labeled D_1(ROCCSD), is analogous to the single-substitution-based D_1(CCSD) for closed-shell systems. The D_1 diagnostics are independent of system size, have the same invariance properties as the energy with respect to orbital rotations, and are easily computed. The magnitude of the D_1(ROCCSD) diagnostic has been shown to correlate with the performance of the CCSD method for the prediction of structures and harmonic vibrational frequencies for 34 molecules. Our results indicate that for values of $D_1(\mathrm{ROCCSD}) \leqslant 0.025$, the quality of the CCSD results are, in general, excellent, whereas values of $D_1(\mathrm{ROCCSD}) > 0.025$ signal an inadequacy in the CCSD approach. The D_1 diagnostics have also been found to correlate well with errors in the CCSD ST splittings. In conclusion, the D_1(ROCCSD) diagnostic is a useful indicator for the quality of properties predicted by ROHF-CCSD theory.

Acknowledgements

The authors would like to thank Prof. J.F. Stanton of the University of Texas, Austin, for providing the ACESII package. Sandia is a multiprogram laboratory operated by Sandia Corporation, a Lockheed Martin Company, for the US Department of Energy under Contract DE-AC04-94AL85000.

References

[1] R.J. Bartlett, in: D.R. Yarkony (Ed.), Modern Electronic Structure Theory, vol. 2, Part 2, World Scientific, Singapore, 1995.
[2] T.J. Lee, G.E. Scuseria, in: S.R. Langhoff (Ed.), Quantum Mechanical Electronic Strucuture Calculations with Chemical Accuracy, Kluwer Academic Publ., Dordrecht, 1995, pp. 47–108.
[3] T.D. Crawford, H.F. Schaefer, in: K.B. Lipkowitz, D.B. Boyd (Eds.), Reviews in Computational Chemistry, vol. 14, chapter 2, VCH Publ., New York, 1999, pp. 33–136.
[4] K.A. Peterson, T.H. Dunning Jr., J. Phys. Chem. 99 (1995) 3898.
[5] K.A. Peterson, T.H. Dunning Jr., J. Mol. Struct. 400 (1997) 93.
[6] T. Helgaker, W. Klopper, H. Koch, J. Noga, J. Chem. Phys. 106 (1997) 9639.
[7] A.G. Császár, W.D. Allen, H.F. Schaefer, J. Chem. Phys. 108 (1998) 9751.
[8] D. Feller, K.A. Peterson, J. Chem. Phys. 108 (1998) 154.
[9] D. Feller, J. Chem. Phys. 111 (1999) 4373.
[10] G. Tarczay, A.G. Császár, M.L. Leininger, W. Klopper, Chem. Phys. Lett. 322 (2000) 119.
[11] C.L. Janssen, I.M.B. Nielsen, Chem. Phys. Lett. 290 (1998) 423.
[12] I.M.B. Nielsen, C.L. Janssen, Chem. Phys. Lett. 310 (1999) 568.
[13] G.H. Golub, C.F. Van Loan, Matrix Computations, 3rd edn., Johns Hopkins University Press, Baltimore, MD, 1996.
[14] D. Jayatilaka, T.J. Lee, J. Chem. Phys. 98 (1993) 9734.
[15] T.H. Dunning Jr., J. Chem. Phys. 90 (1989) 1007.
[16] D.E. Woon, T.H. Dunning Jr., J. Chem. Phys. 98 (1993) 1258.
[17] J.F. Stanton, J. Gauss, J.D. Watts, W.J. Lauderdale, R.J. Bartlett, Int. J. Quantum Chem. Symp. 26 (1992) 879.
[18] T.J. Lee, P.R. Taylor, Int. J. Quantum Chem. Symp. 23 (1989) 199.
[19] T.J. Lee, J.E. Rice, G.E. Scuseria, H.F. Schaefer, Theor. Chim. Acta 75 (1989) 81.
[20] PSI 3.0, T.D. Crawford, et al., PSITECH Inc., Watkinsville, GA, 1999.
[21] K.P. Huber, G. Herzberg, Molecular Spectra and Molecular Structure IV. Constants of Diatomic Molecules, Van Nostrand Reinhold, London, 1979.
[22] Landolt-Börnstein Numerical Data and Functional Relations in Science and Technology, New Series, vol. II/15, Structure Data of Free Polyatomic Molecules, Springer, Berlin, 1987.
[23] K.A. Peterson, J. Chem. Phys. 102 (1995) 262.
[24] D.C. Comeau, I. Shavitt, P. Jensen, P.R. Bunker, J. Chem. Phys. 90 (1989) 6491.